VOL. 13 NO. 9,
AUGUST, 2026
E-ISSN 3026-958X
P-ISSN 3027-1169

African Scholar Publications & Research International
www.africanscholarpub.com

Journal of Science Innovation & Technology Research (JSITR)

Response Surface Optimisation of Material Removal Rate during Wet Lathe Drilling of ASTM A36 Mild Steel Using Central Composite Design

Amanze Gregory Onwuzurike; & John Alabo Michael
Department of Mechanical Engineering, Federal University of Petroleum Resources, Effurun, Nigeria.
Corresponding Author: alabojohn17@gmail.com
DOI: https://doi.org/10.70382/ajsitr.v13i9.079

Abstract

Optimization of the material removal rate (MRR) in wet lathe drilling can improve machining efficiency, while keeping the process parameters under controlled conditions for structural steel applications. Previous studies have explored machinability of ASTM A36 using Taguchi analysis, ANOVA analysis, process-capability analysis, and numerical optimization; however, limited attention has been given to the linear, interaction and quadratic influence of spindle speed, feed rate, and drilling length on MRR under continuous wet lathe drilling conditions with experimental verification. A quadratic model for the MRR was developed and validated and the significant factor effects were established; the optimum conditions for MRR maximization within the design space were determined.; the predictions obtained from the model were verified by experimental trials. For process optimization, 27 experiments were conducted in a randomised central composite design, involving a face-centred arrangement with two replicates for each experimental condition, with rotation included as the fifth factor within defined ranges: spindle speed from 255 to 385 rev/min, feed from 0.177 to 0.303 mm/rev and length of drilling from 44.9 to 60.1 mm. Based on the ANOVA results and prediction error, we developed regression models, using response surface Methodology and Bounded Numerical Optimization method. Fifteen additional runs were subsequently performed independently. The quadratic model was significant. $F(9, 17) = 51.95$ $p < 0.0001$ $R^2 = 0.9649$ Adjusted $R^2 = 0.9463$ and predicted $R^2 = 0.8246$. Spindle speed, drill length, each of the two- factor interactions and the quadratic terms of spindle speed and drilling length were also significant. The numerical optimum occurred at 385 rpm, 0.177 mm /rev, and 56. 040 mm and predicted an MRR of 119.076 mm/s. At the independent verification point, the observed mean was 114.489 ±1.098 mm /s compared with the predicted value of 114. 551 mm /s with a mean percentage prediction error of 0.055 %. The validated response surface provides a practical

basis for selecting productive wet lathe-drilling conditions for ASTM A36 mild steel within the investigated factor ranges.

Keywords: ASTM A36 steel, lathe drilling, material removal rate (MRR), response surface methodology (RSM), central composite design (CCD), process optimization, experimental confirmation.

Introduction

Drilling is a basic hole-making operation in manufacturing, but its productivity depends on coordinated control of the machine, tool, workpiece, and operating conditions. In centre-lathe drilling, the workpiece rotates while the drill advances axially. Spindle speed, feed, drilling length, tool engagement, chip evacuation, and coolant delivery therefore act together. Material removal rate (MRR) expresses the volume removed per unit time and provides a direct measure of process productivity (Tolouei-Rad & Aamir, 2021). Response surface methodology (RSM) is well suited for machining processes in which factor interactions and curvature influence the response. Central composite designs combine factorial, axial, and centre points to estimate a second-order model efficiently. RSM sequence involves selecting influential factors, constructing a design matrix, conducting the experiments, measuring the response, fitting a mathematical model, testing model adequacy through analysis of variance, and interpreting the resulting response surfaces (Philip *et al.*, 2015; Palanikumar, 2021).

ASTM A36 mild steel is widely used in structural fabrication, where drilled holes are required for fastening, assembly, and component integration. Earlier investigations have examined ASTM A36 drilling and turning using Taguchi analysis, ANOVA, process-capability indices, and numerical optimisation (Al Amin *et al.*, 2018; Saha & Majumder, 2018).) studies have also used response surface methodology to model and optimize turning, milling, and boring responses (Izelu *et al.*, 2021; Sarıkaya & Güllü, 2014; Yuvaraju & Nanda, 2018). However, the combined linear, interaction, and quadratic effects of spindle speed, feed, and drilling length on MRR during continuous wet lathe drilling have received limited treatment. The present work also adds replicated experimental confirmation, because model-development statistics alone do not show how consistently a predicted response can be reproduced in a new series of trials. ASTM A36 was selected because of its structural-fabrication relevance; the wet condition was maintained using a fixed soluble-oil flood coolant, and spindle speed, feed, and drilling length represent the rotational, axial-advance, and tool-engagement components of the process.

The study therefore aimed to: (i) develop a quadratic MRR model from a face-centred central composite design; (ii) determine the significant linear, interaction, and curvature effects of spindle speed, feed, and drilling length; (iii) evaluate model adequacy and prediction error; (iv) obtain the MRR-maximising factor combination within the experimental bounds; and (v) confirm the model experimentally through 15 new repetitions at a selected MRR condition.

MATERIALS AND METHODS

Materials, Machine Tool, and Factor Selection

The experiments were conducted on an Elliot Wilson centre lathe (D360 × 1000) using a 10 mm high-speed steel (HSS) twist drill and soluble-oil flood coolant. ASTM A36 mild-steel workpieces measured 50 × 120 mm and were held in a three-jaw chuck, while the drill was mounted in and advanced from the tailstock. Spindle

speed, feed, and drilling length were selected because they represent the rotational, axial-advance, and tool-engagement components of the lathe-drilling process. The ranges were established from the lathe settings, the operating capacity of the 10 mm HSS drill, the workpiece geometry, and tailstock travel; (Izelu *et al.*, 2021; Philip *et al.*, 2015).

Table 1. Experimental factors and levels

Code	Factor	Unit	Low level (-1)	Centre (0)	High level (+1)
A	Spindle speed	rev/min	255	320	385
B	Feed	mm/rev	0.177	0.240	0.303
C	Drilling length	Mm	44.9	52.5	60.1

Table 2. Elemental composition of the ASTM A36 mild-steel workpiece (wt.%)

Material	C	Si	Mn	S	P	Cu	Fe
Mild steel	0.29	0.28	0.10	0.10	0.04	0.20	98.14

Experimental Procedure and MRR Determination

Before each run, the tool height and position relative to the workpiece were standardised using gauges. The factor combinations were applied in the randomised order generated by Design-Expert. Drilling length was set from the tailstock graduations and checked with a FatMax BladeArmor 35 measuring blade. Drilling time was measured with a stopwatch from initial drill-workpiece contact until the specified length was reached, and the drilled-hole diameter was measured with a vernier calliper. The same lathe, drill specification, three-jaw-chuck arrangement, coolant condition, tool-setting procedure, timing definition, and measurement methods were maintained throughout the experiment. Izelu *et al.* (2021) Philip *et al.* (2015). Experimental repeatability was evaluated through the independent 15-repetition confirmation series described in Section 2.5.

For each trial, the removed material was treated as a cylindrical volume determined by the measured hole diameter, D, and drilling length, L:

$$V = \frac{\pi D^2 L}{4} \tag{1}$$

Material removal rate was calculated by dividing the removed volume by the measured drilling time, t:

$$\text{MRR} = \frac{V}{t} = \frac{\pi D^2 L}{4t} \tag{2}$$

where V is removed volume (mm^3), D is measured hole diameter (mm), L is drilling length (mm), t is drilling time (s), and MRR is expressed in mm^3/s.

Central Composite Design and Model Fitting

A randomised face-centred central composite design was generated in Design-Expert 13.0.1.0. The 27-run matrix comprised eight factorial points, six axial points, and 13 centre points. This arrangement provided information for estimating linear effects, all two-factor interactions, and quadratic curvature. (Philip *et al.*, 2015; Palanikumar, 2021;). The general second-order model was:

$$Y = \beta_0 + \beta_1 A + \beta_2 B + \beta_3 C + \beta_{12} AB + \beta_{13} AC + \beta_{23} BC + \beta_{11} A^2 + \beta_{22} B^2 + \beta_{33} C^2 + \varepsilon \tag{3}$$

Here, Y is predicted MRR; A, B, and C are coded levels of spindle speed, feed, and drilling length; β_0 is the intercept; β_1-β_3 are linear coefficients; β_{12}-β_{23} are interaction coefficients; β_{11}-β_{33} are quadratic coefficients; and ε is the residual. Model selection used sequential sums of squares. Adequacy was evaluated using ANOVA, R^2, adjusted R^2, predicted R^2, coefficient of variation, PRESS, adequate

precision, variance-inflation factors, normal probability of residuals, residuals versus predicted values, and predicted-versus-measured agreement. Terms with $p < 0.05$ were considered statistically significant, while hierarchy was retained in the fitted polynomial.

Prediction-error metrics

Predicted MRR values were calculated at all 27 design locations using the fitted actual-factor equation. Prediction error was quantified as follows:

$$\text{MSE} = \frac{1}{n}\sum_{i=1}^{n}\left(Y_i - \hat{Y}_i\right)^2 \tag{4}$$

$$\text{RMSE} = \sqrt{\text{MSE}} \tag{5}$$

$$\text{MAE} = \frac{1}{n}\sum_{i=1}^{n}\left|Y_i - \hat{Y}_i\right| \tag{6}$$

$$\text{MAPE} = \frac{100}{n}\sum_{i=1}^{n}\left|\frac{Y_i - \hat{Y}_i}{Y_i}\right| \tag{7}$$

$$\text{Absolute prediction error} = 100\left|\frac{Y - \hat{Y}}{Y}\right| \tag{8}$$

In these expressions, Y_i and $\hat{Y}_i$ are the measured and predicted MRR values for observation i, and n is the number of observations.

Single-Response Optimisation and Independent Confirmation

The actual-factor equation was maximised subject to the experimental bounds $255 \le N \le 385$ rev/min, $0.177 \le f \le 0.303$ mm/rev, and $44.9 \le L \le 60.1$ mm. A bounded numerical search was performed over the complete factor domain. The solution was verified by evaluating the active boundary conditions and the stationary drilling length obtained from the first derivative of the actual-factor equation. This calculation produced the single-response MRR optimum reported in Section 3.4.

$$\max_{N,f,L} \text{MRR}(N, f, L) \tag{9}$$

$$\text{subject to } 255 \le N \le 385, \quad 0.177 \le f \le 0.303, \quad 44.9 \le L \le 60.1$$

Independent confirmation used a separate MRR model solution at N = 255 rev/min, f = 0.295675 mm/rev, and L = 44.9 mm, for which the fitted equation predicted 114.551 mm^3/s. The feed value is reported as 0.296 mm/rev in the confirmation table. Fifteen new MRR observations were obtained at this condition and were not included in model fitting. Their mean, sample standard deviation, coefficient of variation, and two-sided 95% confidence interval were calculated using:

$$\overline{Y} = \frac{1}{n}\sum_{i=1}^{n} Y_i \tag{10}$$

$$s = \sqrt{\frac{\sum_{i=1}^{n}\left(Y_i - \overline{Y}\right)^2}{n-1}} \tag{11}$$

$$\text{CV} = 100\frac{s}{\overline{Y}} \tag{12}$$

$$95\%\ \text{CI} = \overline{Y} \pm t_{0.975,n-1}\frac{s}{\sqrt{n}} \tag{13}$$

For n = 15, $t_{0.975,14} = 2.145$. The predicted value was compared with the 15 observations using MAE, RMSE, MAPE, mean prediction error, and maximum individual percentage error. Confirmation was considered satisfactory when the mean prediction error and replicate CV were each below 5%.

Results

Central composite design observations

Table 3. Central composite design matrix and measured MRR

Run	Spindle speed (rev/min)	Feed (mm/rev)	Drilling length (mm)	Measured MRR (mm^3/s)
1	320	0.240	52.5	104.74
2	320	0.240	52.5	104.74
3	320	0.240	52.5	104.74
4	385	0.240	52.5	102.19
5	385	0.303	44.9	99.87
6	320	0.240	52.5	104.74
7	320	0.240	52.5	104.74
8	320	0.240	52.5	104.74
9	320	0.240	52.5	104.74
10	320	0.303	52.5	101.49
11	255	0.177	60.1	65.87
12	320	0.240	44.9	98.21
13	255	0.240	52.5	84.67
14	320	0.240	52.5	104.74
15	255	0.177	44.9	79.34
16	320	0.240	52.5	104.74
17	385	0.303	60.1	83.67
18	320	0.240	52.5	104.74
19	320	0.240	60.1	79.63
20	320	0.240	52.5	104.74
21	320	0.240	52.5	104.74
22	385	0.177	60.1	116.7
23	320	0.240	52.5	104.74
24	255	0.303	60.1	65.794
25	385	0.177	44.9	99.08
26	320	0.177	52.5	100.71
27	255	0.303	44.9	118.98

Measured MRR ranged from 65.794 to 118.98 mm^3/s. The highest measured response occurred at 255 rev/min, 0.303 mm/rev, and 44.9 mm. The 13 centre-point observations were recorded as 104.74 mm^3/s to two decimal places.

Quadratic model, ANOVA, and Regression Equations

Sequential model testing supported the quadratic form: the additional quadratic contribution was significant ($p < 0.0001$), while the cubic form was aliased. The quadratic model was significant, $F(9, 17) = 51.95$, $p < 0.0001$, and explained 96.49% of the observed variation in MRR.

Table 4. Analysis of variance for the quadratic MRR model

Source	SS	Df	MS	F	p
Model	4395.46	9	488.38	51.95	<0.0001
A: Spindle speed	754.40	1	754.40	80.25	<0.0001
B: Feed	6.57	1	6.57	0.70	0.4148
C: Drilling length	702.51	1	702.51	74.73	<0.0001
AB	644.48	1	644.48	68.56	<0.0001
AC	579.29	1	579.29	61.62	<0.0001
BC	675.94	1	675.94	71.90	<0.0001
A^2	84.84	1	84.84	9.02	0.0080
B^2	13.32	1	13.32	1.42	0.2503
C^2	281.31	1	281.31	29.92	<0.0001
Residual	159.81	17	9.40		
Lack of fit	159.81	5	31.96		-
Pure error	0.00	12	0.00		
Corrected total	4555.27	26			

Spindle speed (A), drilling length (C), all two-factor interactions (AB, AC, and BC), and the quadratic terms A^2 and C^2 were significant. Feed did not have a significant isolated main effect, but its participation in the significant AB and BC terms shows that its influence depended on spindle speed and drilling length.

Table 5. Coefficients of the coded quadratic model

Term	Estimate	SE	95% CI low	95% CI high	VIF	p
Intercept	103.37	0.7797	101.73	105.02	-	-
A	8.6856	0.9696	6.64	10.73	1.00	<0.0001
B	0.8104	0.9696	-1.24	2.86	1.00	0.4148
C	-8.3816	0.9696	-10.43	-6.34	1.00	<0.0001
AB	-8.9755	1.0840	-11.26	-6.69	1.00	<0.0001
AC	8.5095	1.0840	6.22	10.80	1.00	<0.0001
BC	-9.1920	1.0840	-11.48	-6.90	1.00	<0.0001
A^2	-5.4935	1.8287	-9.35	-1.64	2.24	0.0080
B^2	2.1765	1.8287	-1.68	6.03	2.24	0.2503
C^2	-10.0035	1.8287	-13.86	-6.15	2.24	<0.0001

The fitted coded-factor equation was:

$$\text{MRR} = 103.3714 + 8.6856A + 0.8104B - 8.3816C - 8.9755AB + 8.5095AC - 9.1920BC - 5.4935A^2 + 2.1765B^2 - 10.0035C^2 \quad (14)$$

The corresponding equation in actual factor units was:

$$\text{MRR} = -584.322786 + 0.587457N + 1458.91594f + 16.177415L - 2.191819Nf + 0.017226NL - 19.197995fL - 0.001300N^2 + 548.384307f^2 - 0.173190L^2 \quad (15)$$

where N is spindle speed (rev/min), f is feed (mm/rev), and L is drilling length (mm).

Model adequacy, diagnostics, and prediction accuracy

Table 6. Model-adequacy and comparison statistics

Statistic	Value
Standard deviation	3.066 mm^3/s
Mean response	98.438 mm^3/s

Statistic	Value
Coefficient of variation	3.115%
R^2	0.9649
Adjusted R^2	0.9463
Predicted R^2	0.8246
Adequate precision	28.5937
PRESS	799.09
BIC	157.59
AICc	158.38

The difference between adjusted and predicted R^2 was 0.1217, while adequate precision was above the reference value of 4. All VIF values were 2.24 or lower. The normal-probability plot followed the reference line closely, the residual-versus-predicted plot showed no systematic structure, and predicted MRR values tracked the measured values across the design space. These diagnostics are shown in Figure 1, while the one-factor, interaction, contour, and response-surface are presented in Figures 2–5.

Table 7. Prediction-error statistics for the 27 design points

Validation quantity	Result
Number of design points	27
MSE	5.919 $(mm^3/s)^2$
RMSE	2.433 mm^3/s
MAE	1.977 mm^3/s
MAPE	2.079%
Nearest tested condition to the confirmation point	255 rev/min; 0.303 mm/rev; 44.9 mm
Predicted MRR at nearest condition	117.234 mm^3/s
Measured MRR at nearest condition	118.98 mm^3/s
Absolute prediction error	1.467%

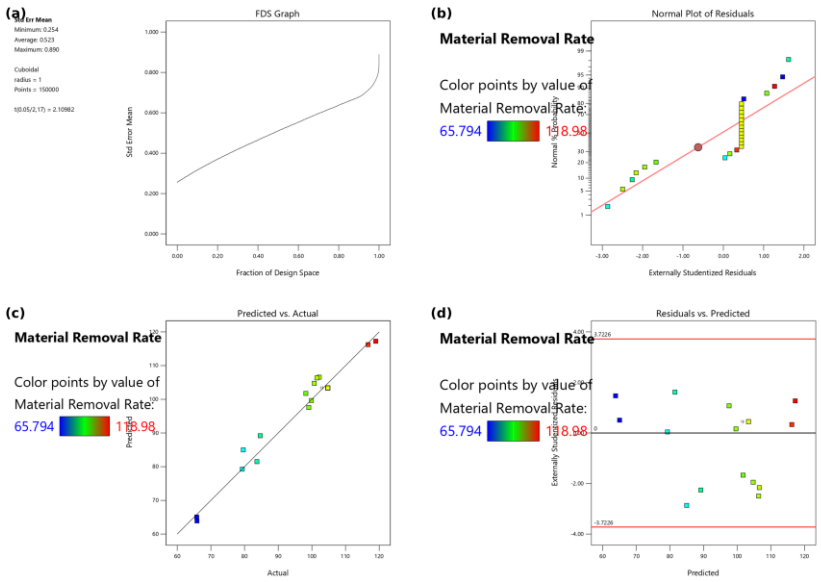


Figure 1: Design-Expert MRR model diagnostics: (a) fraction-of-design-space graph; (b) normal probability plot of externally studentised residuals; (c) predicted versus actual MRR; and (d) residuals versus predicted MRR.

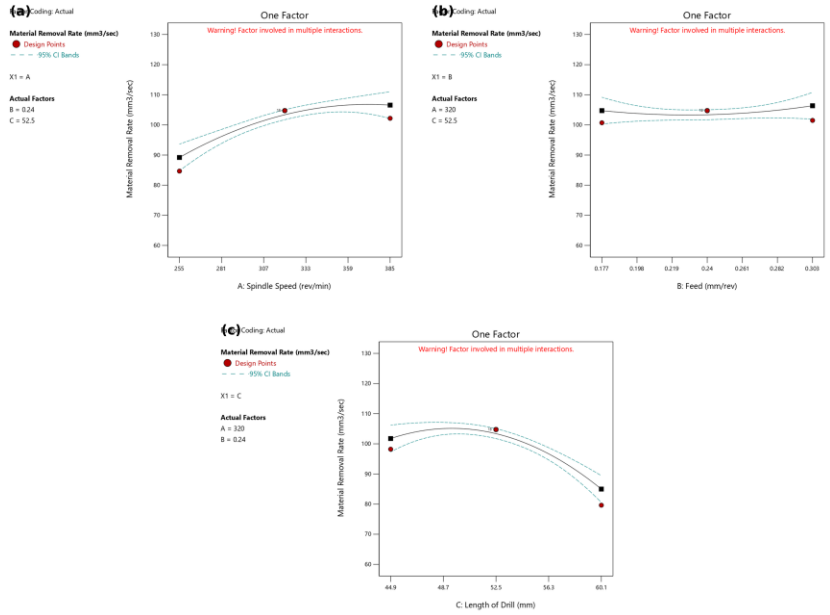


Figure 2: Design-Expert one-factor plots for predicted MRR: (a) spindle speed; (b) feed; and (c) drilling length.

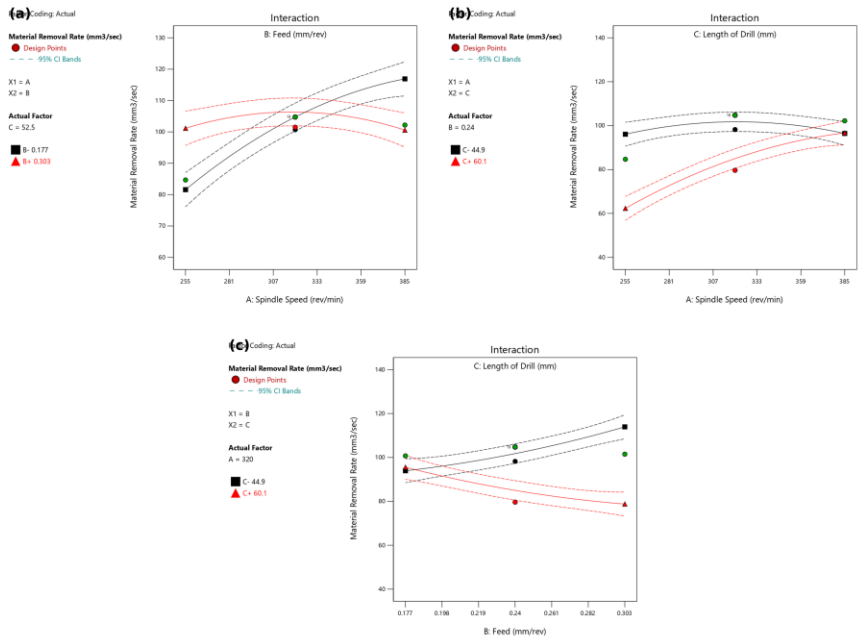


Figure 3: Design-Expert two-factor interaction plots for MRR: (a) spindle speed × feed; (b) spindle speed × drilling length; and (c) feed × drilling length.

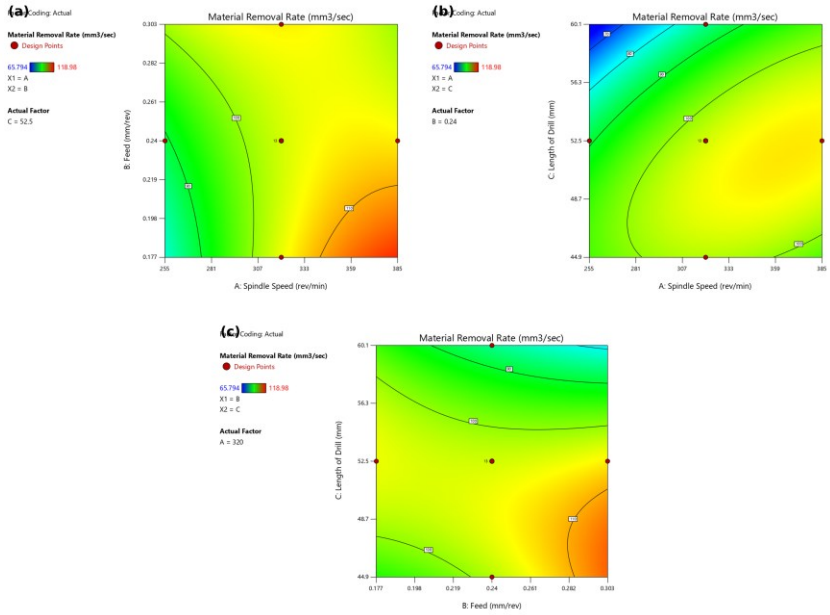


Figure 4: Design-Expert contour plots for predicted MRR: (a) spindle speed and feed; (b) spindle speed and drilling length; and (c) feed and drilling length.

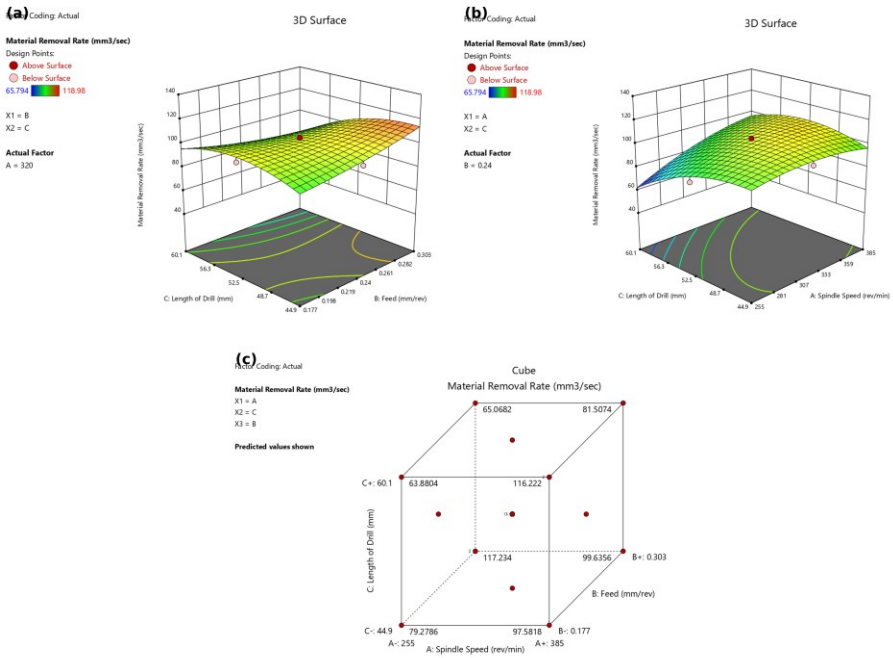


Figure 5: Design-Expert response-surface outputs for MRR: (a) drilling length–feed surface; (b) drilling length–spindle speed surface; and (c) cube representation of the experimental factor space.

Numerical MRR Optimum and Independent Confirmation

Bounded maximisation of the actual-factor equation identified N = 385 rev/min, f = 0.177 mm/rev, and L = 56.040 mm as the single-response MRR optimum. The corresponding predicted MRR was 119.076 mm^3/s. The optimum occurred at the upper spindle-speed boundary, the lower feed boundary, and an interior drilling length. Substitution of N = 385 and f = 0.177 into the first derivative with respect to L gave L = 56.040 mm, confirming the numerical solution.

Table 8. Single-response optimisation result and independent confirmation condition

Quantity	Single-response optimum	Independent confirmation condition
Spindle speed	385 rev/min	255 rev/min
Feed	0.177 mm/rev	0.295675 mm/rev (reported as 0.296)
Drilling length	56.040 mm	44.9 mm
Predicted MRR	119.076 mm^3/s	114.551 mm^3/s
Purpose	Maximum of the MRR-only equation	Replicated experimental check of model prediction

The 15 independent confirmation results are reported in Table 9. The optimizer feed of 0.295675 mm/rev is shown as 0.296 mm/rev. Individual absolute percentage errors ranged from 0.071% to 1.516%. Table 9. Show the confirmation observations at the selected high-MRR condition

Table 9. confirmation observations at the selected high-MRR condition

Run	Speed (rev/min)	Feed (mm/rev)	Length (mm)	MRR (mm^3/s)	Absolute error (%)
1	255	0.296	44.9	112.84	1.516
2	255	0.296	44.9	115.76	1.044
3	255	0.296	44.9	114.22	0.290
4	255	0.296	44.9	113.51	0.917
5	255	0.296	44.9	116.03	1.275
6	255	0.296	44.9	114.89	0.295
7	255	0.296	44.9	112.97	1.400
8	255	0.296	44.9	115.18	0.546
9	255	0.296	44.9	113.86	0.607
10	255	0.296	44.9	114.64	0.078
11	255	0.296	44.9	116.21	1.427
12	255	0.296	44.9	113.28	1.122
13	255	0.296	44.9	114.47	0.071
14	255	0.296	44.9	115.52	0.839
15	255	0.296	44.9	113.95	0.528

Table 10. Statistical summary of the independent confirmation observations

Statistic	MRR result
Model prediction	114.551 mm^3/s
Experimental mean	114.489 mm^3/s
Sample standard deviation	1.098 mm^3/s
Coefficient of variation	0.959%
95% confidence interval	113.881-115.097 mm^3/s
Mean prediction error	0.055%

Statistic	MRR result
MAE	0.912 mm^3/s
RMSE	1.063 mm^3/s
MAPE	0.797%
Maximum individual error	1.516%
Confirmation criterion	Met (mean error < 5%; CV < 5%)

The predicted MRR is within the 95% confidence interval of the replicated mean. The experimental mean differed from the prediction by 0.062 mm^3/s, or 0.055%. The CV was below 1%, and all confirmation error measures were lower than the corresponding errors calculated across the 27 model-development points.

DISCUSSION

The quadratic response surface represented the MRR data effectively. The model explained 96.49% of the observed variation, and the adjusted and predicted R^2 values remained reasonably close. Adequate precision of 28.5937 demonstrated a strong signal relative to model noise. The 27-point RMSE of 2.433 mm^3/s and MAPE of 2.079% provide additional evidence that the fitted equation followed the measured response within the experimental region. These findings agree with the modelling sequence used by Philip *et al.* (2015), in which a quadratic response surface was selected through model comparison, tested through ANOVA, and examined through residual and predicted-versus-measured plots.

The significant interaction terms explain why MRR cannot be interpreted from isolated main effects alone. Spindle speed and drilling length were significant as individual factors, whereas feed became important through its interactions with spindle speed and drilling length. The response surfaces therefore changed direction across different factor combinations. This behaviour supports the use of RSM rather than one-factor-at-a-time experimentation and is consistent with machining studies that used interaction and quadratic terms to represent parameter dependence (Izelu *et al.*, 2021; Sarıkaya & Güllü, 2014; Yuvaraju & Nanda, 2018).

The MRR-only optimum of 385 rev/min, 0.177 mm/rev, and 56.040 mm differs from the highest measured design point, which occurred at 255 rev/min, 0.303 mm/rev, and 44.9 mm. The two responses were nevertheless close: 119.076 mm^3/s predicted at the numerical optimum and 118.98 mm^3/s measured at the highest design point. This result reflects the strong AB, AC, and BC interactions and the negative curvature in spindle speed and drilling length. Izelu *et al.* (2021) likewise demonstrated RSM-based modelling and optimisation for a dry hard-boring process, but their optimum conditions related to a different material, tool, response set, and factor domain. Al Amin *et al.* (2018) reported a low-RPM/high-feed direction for improved surface roughness under their ASTM A36 drilling conditions. By contrast, Saha and Majumder (2018) reported an optimum for average surface roughness at 240 rev/min, 0.16 mm/rev, and 0.1 mm depth of cut in ASTM A36 turning. These studies considered different responses and machining configurations and therefore provide contextual comparison rather than direct confirmation of the present MRR optimum. The independent confirmation series provides a direct test of the fitted equation using observations that were not part of model estimation. At the selected high-MRR condition, the mean response of 114.489 mm^3/s was only 0.055% from the prediction of 114.551 mm^3/s and the predicted value lay within the 95% confidence interval. The CV of 0.959% and maximum individual error of 1.516% demonstrate stable repetition. The agreement between the confirmation series and the model strengthens confidence in using the response surface for process-parameter selection.

The study combines statistical modelling, numerical optimisation, and replicated experimental confirmation in one workflow. The resulting equation provides a practical basis for selecting productive wet lathe-drilling settings for ASTM A36 steel within the investigated domain.

CONCLUSION

A randomised 27-run face-centred central composite design produced a statistically significant quadratic model for MRR during wet centre-lathe drilling of ASTM A36 mild steel. The model achieved $R^2 = 0.9649$, adjusted $R^2 = 0.9463$, predicted $R^2 = 0.8246$, CV = 3.11%, and adequate precision = 28.5937. Spindle speed, drilling length, all pairwise interactions, and the quadratic terms of spindle speed and drilling length were significant. The design-point RMSE, MAE, and MAPE were 2.433 mm^3/s, 1.977 mm^3/s, and 2.079%, respectively. Single-response maximisation identified 385 rev/min, 0.177 mm/rev, and 56.040 mm as the numerical optimum, with predicted MRR = 119.076 mm^3/s. At the independent confirmation condition of 255 rev/min, 0.296 mm/rev, and 44.9 mm, 15 repetitions produced 114.489 ± 1.098 mm^3/s compared with the model prediction of 114.551 mm^3/s. The mean prediction error was 0.055%, CV was 0.959%, MAPE was 0.797%, and the maximum individual error was 1.516%. The close agreement between measured and predicted values confirms the predictive accuracy of the quadratic response surface and demonstrates its value for selecting productive wet lathe-drilling conditions within the investigated factor ranges. Future studies can extend the framework to tool life, finished-hole geometry, surface integrity, energy demand, and alternative coolant strategies.

DATA AVAILABILITY

All numerical data used for model development, optimisation, and experimental confirmation are reported in Tables 3, 8, and 9 of this manuscript.

REFERENCES

Al Amin, M., Rifat, U. A., Rahman, M. H., & Kibria, M. G. (2018). Performance analysis of mild steel (ASTM A36) under varying drilling conditions using Taguchi and ANOVA. *Global Journal of Researches in Engineering: J General Engineering, 18*(3), 7–15.

Izelu, C. O., Essien, E. I., Okwu, M. O., Garba, D. K., & Agunobi-Ozoekwe, C. N. (2021). Lathe boring operation on ASTM A304 steel parameter optimization using response surface methodology. *Australian Journal of Mechanical Engineering, 19*(5), 544–558. https://doi.org/10.1080/14484846.2019.1662534

Palanikumar, K. (2021). Introductory chapter: Response surface methodology in engineering science. In K. Palanikumar (Ed.), *Response surface methodology in engineering science*. IntechOpen. https://doi.org/10.5772/intechopen.100484

Philip, S. D., Chandramohan, P., & Rajesh, P. K. (2015). Prediction of surface roughness in end milling operation of duplex stainless-steel using response surface methodology. *Journal of Engineering Science and Technology, 10*(3), 340–352.

Saha, A., & Majumder, H. (2018). Performance analysis and optimization in turning of ASTM A36 through process capability index. *Journal of King Saud University – Engineering Sciences, 30*(4), 377–383. https://doi.org/10.1016/j.jksues.2016.11.002

Sarıkaya, M., & Güllü, A. (2014). Taguchi design and response surface methodology-based analysis of machining parameters in CNC turning under MQL. *Journal of Cleaner Production, 65*, 604–616. https://doi.org/10.1016/j.jclepro.2013.08.040

Tolouei-Rad, M., & Aamir, M. (2021). Analysis of the performance of drilling operations for improving productivity. In M. Tolouei-Rad (Ed.), *Drilling technology* (pp. 1–16). IntechOpen. https://doi.org/10.5772/intechopen.96497

Yuvaraju, B. A. G., & Nanda, B. K. (2018). Prediction of vibration amplitude and surface roughness in boring operation by response surface methodology. *Materials Today: Proceedings, 5*(2), 6906–6915. https://doi.org/10.1016/j.matpr.2017.11.352